



Revista Mexicana de Física

ISSN: 0035-001X

rmf@ciencias.unam.mx

Sociedad Mexicana de Física A.C.

México

Rickards, J.

The lumped heat capacity method applied to target heating

Revista Mexicana de Física, vol. 59, núm. 4, julio-agosto, 2013, pp. 328-334

Sociedad Mexicana de Física A.C.

Distrito Federal, México

Available in: <http://www.redalyc.org/articulo.oa?id=57027861008>

- How to cite
- Complete issue
- More information about this article
- Journal's homepage in redalyc.org

redalyc.org

Scientific Information System

Network of Scientific Journals from Latin America, the Caribbean, Spain and Portugal

Non-profit academic project, developed under the open access initiative

The lumped heat capacity method applied to target heating

J. Rickards

*Instituto de Física, Universidad Nacional Autónoma de México,
Apartado Postal 20364, México 01000, D.F.*

Received 20 March 2012; accepted 14 March 2013

The temperature of metal samples was measured while they were bombarded by the beam from the a particle accelerator. The evolution of the temperature with time can be explained using the lumped heat capacity method of heat transfer. A strong dependence on the type of mounting was found.

Keywords: Target heating; accelerator.

Se midió la temperatura de muestras metálicas al ser bombardeadas por el haz de iones del Acelerador Pelletron del Instituto de Física. La evolución de la temperatura con el tiempo se puede explicar usando el método de capacidades acumuladas de transferencia de calor. Se encontró una marcada dependencia en el tipo de montura de la muestra.

Descriptores: Calentamiento blanco; acelerador.

PACS: 06.60.Ei; 29.20.Ba

1. Introduction

When the ion beam from a particle accelerator strikes a solid sample, it deposits its energy in different ways. If the energy is of the order of a few MeV, the mechanisms of energy loss (stopping power) can be separated into interactions with electrons, which produce ionization or atomic excitation, and interactions with the whole atoms, producing atomic displacements and structural damage. In both processes secondary radiation is generated (photons, electrons, atoms) which gives rise to avalanches in which eventually the energy is dissipated until it reaches the thermal regime. The sample is heated; only a small fraction of the energy, like emitted radiation and energy absorbed in chemical bonding, does not contribute to a rise in temperature.

For a typical beam size and current, the arrival of each individual particle is an isolated event, both in time and in space. The primary event takes place in times of the order of 10^{-15} s, followed by pre-thermal processes until about 10^{-12} s, when one may consider that thermal processes begin. The primary ion trajectory where the energy is deposited has dimensions of some nm to some μm , depending on type of ion and its energy; eventually the effects travel to larger regions. For large times, of the order of a few seconds, microscopic processes evolve into heating of the whole sample, and hence macroscopic effects.

Since heating the sample could affect its properties, it is important to study the temperature and how it evolves in time, which is the object of the present report. The procedure followed is applicable also to electron microscopy, given the similar geometries and orders of magnitude involved.

2. Experiment

In an ion implantation experiment, or in sample analysis using nuclear methods, the sample is normally mounted on a

holder which is in turn in contact with other parts of the equipment, like a goniometer or a Faraday cup, all within a vacuum chamber. Heat is transferred from the beam spot through the sample to the holder and then to the rest of the system.

Our initial experiment consisted of measuring the temperature at the surface of a cylindrical sample of 316L stainless steel of 1 cm diameter and 0.5 cm height, as it was bombarded with a 4 MeV, 1 mm diameter, proton beam from the Instituto de Física 9SDH-2 Pelletron Accelerator. The sample was attached to an aluminum holder with small metallic flaps. A thermocouple was used to measure the temperature, placed on the front face of the sample in a small hole about 5 mm away from the beam spot. Due to the electrical contact of the thermocouple, the beam current was not measured

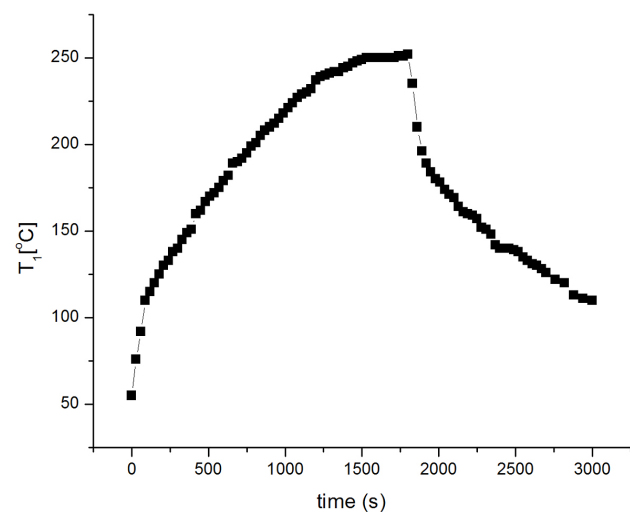


FIGURE 1. An example of the evolution of the temperature of a 316L stainless steel sample bombarded by a 4 MeV, 500 nA proton beam.

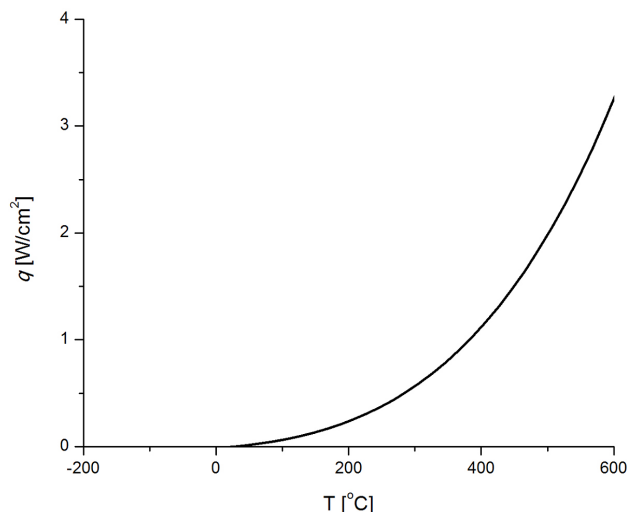


FIGURE 2. Behavior of radiation heat loss q with temperature in $^{\circ}\text{C}$; $T_2 = 300\text{ }^{\circ}\text{K}$.

directly. Rather it was fixed initially at 500 nA and then controlled with a beam profile monitor before the scattering chamber. Temperature measurements were taken in 30 second intervals during 30 minutes with the beam on, and then the beam was cut off to observe the cooling process. Figure 1 shows typical results: the temperature rises at a certain rate, then there is a change in slope, and a tendency to saturate. When the beam is removed, first there is a fast drop in temperature and then a change in slope to slower cooling.

Some typical numbers for the application of heat transfer concepts are: for a 1 MeV energy, 1 μA current beam, the power transmitted to the sample is $\text{J/s} = 1\text{ W}$, since $1\text{ }\mu\text{A} = 6.24 \times 10^{12}$ projectiles/s and each projectile deposits $1.6 \times 10^{-13}\text{ J}$. The rate of heat transfer is q has units of power [$\text{J/s} = \text{W}$]. For a scanning electron microscope, typical values would be 100 μA at 20 keV = 2 W.

3. Heat transfer

The heat transfer mechanisms are convection, conduction and radiation. In the present case, due to vacuum, there is no convection. Conduction is to all objects in contact with the sample, and radiation is mainly to the walls of the vacuum chamber.

The power lost by **radiation** is obtained from

$$q = \sigma A (T_1^4 - T_2^4), \tag{1}$$

where σ is $5.669 \times 10^{-8}\text{ W/m}^2\text{ }^{\circ}\text{K}^4$ is the Stefan-Boltzmann constant and is independent of the material and the beam. The radiating area is A , and T_1 , T_2 are the temperatures of the radiator and the absorber, respectively. For the present case, the power lost by radiation is shown in Fig. 2, with $T_2 = 300\text{ }^{\circ}\text{K}$. Due to its relatively low values in the temperature interval of interest, it will be neglected.

To describe **conduction** in one dimension, if q is the rate of heat transfer in [$\text{W} = \text{J/s}$], and A is the area over which

heat is transferred), in the stationary case the heat transferred per unit area is proportional to the temperature gradient. Heat conduction in solids is described [1] by Eq. (2), where q is the rate of heat transfer [W], k is the thermal conductivity of the material [$\text{W/m }^{\circ}\text{C}$], ρ is its density, c is the specific heat [$\text{J/kg }^{\circ}\text{C}$] and $\alpha = k / \rho c$ is the thermal diffusivity.

$$\nabla^2 T + \frac{1}{k} \frac{\partial q}{\partial \tau} = \frac{\rho c}{k} \frac{\partial T}{\partial \tau} = \frac{1}{\alpha} \frac{\partial T}{\partial \tau}. \tag{2}$$

With the proper boundary conditions expressions can be derived [1] for the spatial distribution of temperature with time. For the present case, since the particle beam strikes a plane surface on the sample, the one-dimensional flow in a semi-infinite solid was selected. For stainless steel: $c = 460\text{ J/kg }^{\circ}\text{C}$, $\alpha = 0.444 \times 10^{15}\text{ m}^2/\text{s}$, $k = 16.3\text{ W/m }^{\circ}\text{C}$ at 0°C , $\rho = 7.98\text{ g/cm}^3$. With these values one can calculate that the temperature at the back of the sample will reach 0.368 of the temperature at the front in approximately 2 s.

4. Temperature measurements with different mountings

Temperature measurements were made on 316L stainless steel samples mounted in different ways on an aluminum holder. Three different mountings are shown in Fig. 3. The first (A) corresponds to the sample mounted on the holder with metallic flaps. In mounting B conducting silver paint was added. In mounting C the sample was placed inside a cup in a thick aluminum holder. The three mountings produced different results, indicated in Fig. 4. Case A shows a rapid heating followed by a slower region; in cooling there is also a change in slope. In case B the heating is slower, with no change in slope; cooling shows no change in slope. Finally, in case C there is a change in slope on heating, but when the beam is removed the sample temperature rises slightly before cooling down.

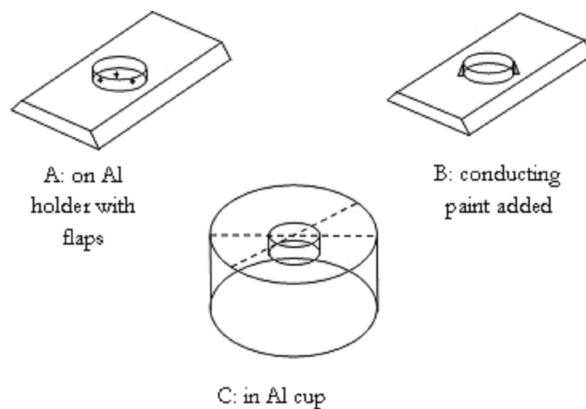


FIGURE 3. The three different mountings used in these experiments.

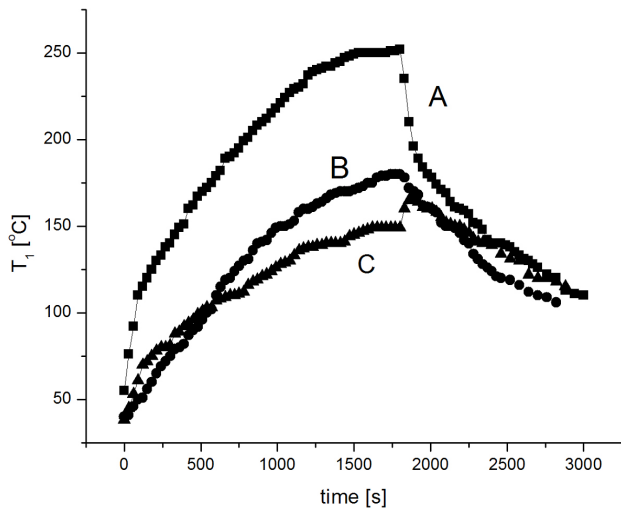


FIGURE 4. Evolution of temperature using the three mountings A, B and C.

5. Application of the lumped heat capacity method

In order to explain the unexpected temperature behavior, the lumped heat capacity method [2] was used. In this method an analogy with an electric circuit of the system of two materials in contact (the sample and the holder), the first of which receives an energy q (inset Fig. 5).

In the electric circuit nodes T_1 and T_2 (see Fig. 5) represent the sample and the holder. Both temperatures T_1 and T_2 are assumed constant. This is valid for small conducting objects, as in our case. In the experiment the temperature measurements were made over large times of many minutes, whereas the calculations using Eq. (2) indicated that the characteristic times in our case are several seconds, so this is considered a good approximation. The node T_∞ (ground) represents room temperature.

Capacitors C_1 and C_2 represent the increase of internal energy of the sample and the holder, respectively. In each case $C = \rho cV$, where ρ is the density, c is the specific heat, and V is the volume. Resistance R_1 represents the contact between sample and holder, including the flaps, and R_2 represents the contact between the holder and the rest of the system. The power supply corresponds to the heat supply q .

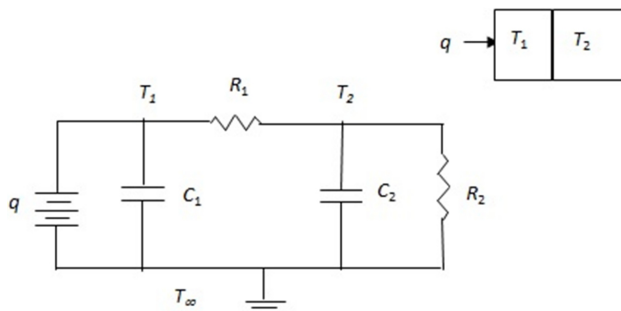


FIGURE 5. The thermal system (inset) and the equivalent electric circuit used to analyze it.

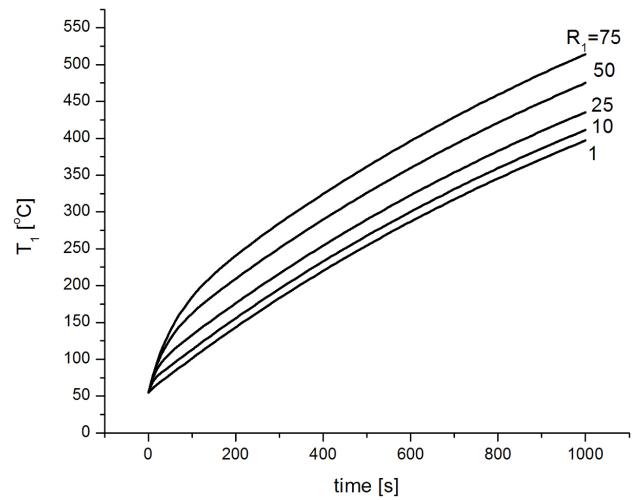


FIGURE 6. Calculated dependence of the sample temperature on the contact resistance R_1 between sample and holder, with all other parameters fixed.

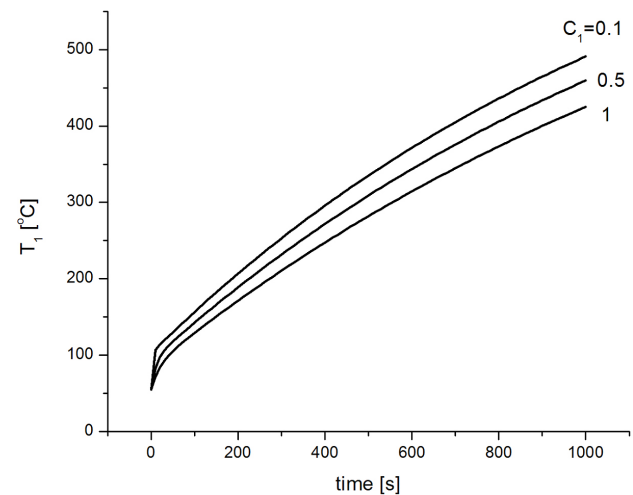


FIGURE 7. Calculated dependence of the sample temperature on C_1 , which is proportional to the density, the specific heat, and the volume of the sample. All other parameters are fixed.

The energy balance at each of the nodes gives

$$\left. \begin{aligned} q &= \frac{1}{R_1}(T_1 - T_2) + C_1 \frac{\partial T_1}{\partial \tau} \\ \frac{1}{R_1}(T_2 - T_1) + \frac{1}{R_2}(T_2 - T_\infty) &= -C_2 \frac{\partial T_2}{\partial \tau} \end{aligned} \right\} \quad (3 \text{ a,b})$$

In Eq. (3a), the energy flow in the sample, the first term on the right is the flow to the holder across the contact resistance; the second term is the energy used to heat the sample. In Eq. (3b), for the holder, the member on the left is the heat flow to the sample and to the system, respectively, and the right member represents the heating of the holder.

During **heating** the initial conditions are: for $\tau = 0$, $T_1 = T_2 = T_\infty$.

The solutions can be written as:

$$\left. \begin{aligned} T_1 &= T'_\infty + Me^{m_1 \tau} + Ne^{m_2 \tau} \\ T_2 &= T_1 + \frac{Mm_1}{K_1} e^{m_1 \tau} + \frac{Nm_2}{K_1} e^{m_2 \tau} - qR_1 \end{aligned} \right\} \quad (4 \text{ a,b})$$

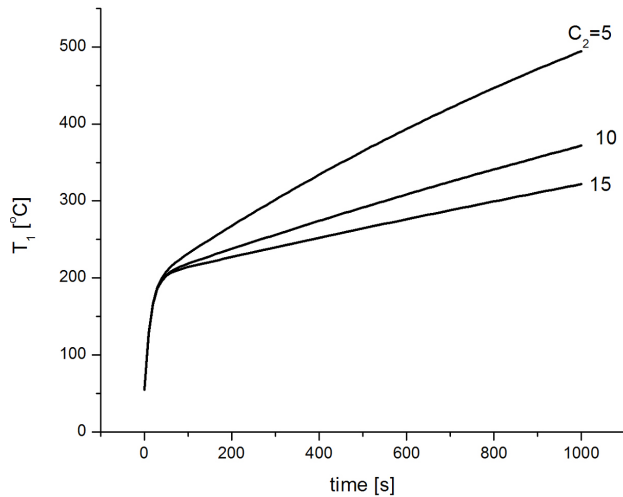


FIGURE 8. Calculated dependence of the sample temperature on C_2 , which is proportional to the density, the specific heat, and the volume of the holder. All other parameters are fixed.

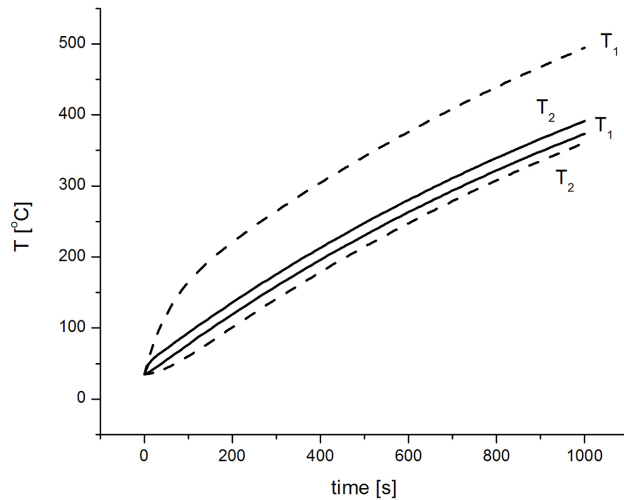


FIGURE 9. Calculated temperatures of the sample (T_1) and the holder (T_2). Solid lines correspond to a small value of R_1 ; dashed lines correspond to a large value of R_1 .

We define the constants $K_1=1/R_1C_1$, $K_2=1/R_1C_2$, $K_3=1/R_2C_2$. In terms of these constants

$$T'_\infty = T_\infty + \frac{K_2 + K_3}{K_1 K_3} \frac{q}{C_1} \tag{5}$$

$$\left. \begin{aligned} m_1 &= \frac{-(K_1+K_2+K_3) + \sqrt{(K_1+K_2+K_3)^2 - 4K_1K_3}}{2} \\ m_2 &= \frac{-(K_1+K_2+K_3) - \sqrt{(K_1+K_2+K_3)^2 - 4K_1K_3}}{2} \end{aligned} \right\} \tag{6 a,b}$$

$$\left. \begin{aligned} M &= \frac{q}{C_1} \frac{1}{m_1 - m_2} \left[1 + \frac{K_2 + K_3}{K_1 K_3} m_2 \right] \\ N &= -\frac{K_2 + K_3}{K_1 K_3} \frac{q}{C_1} - \frac{q}{C_1} \frac{1}{m_1 - m_2} \left[1 + \frac{K_2 + K_3}{K_1 K_3} m_2 \right] \end{aligned} \right\} \tag{7 a,b}$$

Using these expressions the temperature evolution of the sample T_1 was calculated and how it depends on the parameters R_1 , C_1 and C_2 . The dependence on R_1 is shown in Fig. 6, with all other parameters fixed. For large values of R_1 the temperature of the sample is higher than for smaller values. This is expected, since the heat flow to the holder is inhibited. Also, for large values of R_1 there is a change of slope associated with the initial heating of only the sample. Small values of R_1 imply a good thermal contact between sample and holder, so they both heat up simultaneously and there is no change of slope.

The dependence on C_1 , which is proportional to the specific heat of the sample, is shown in Fig. 7. Low values of C_1 mean that the sample heats up rapidly, and after the change of slope both sample and holder are heated. For large values the sample heats up more slowly.

The dependence on C_2 , which is proportional to the specific heat and the volume of the holder, is shown in Fig. 8. If the specific heat is large, after the change of slope the sample and holder heat up slowly; for small values heating is faster.

Figure 9 shows the calculated temperatures of the sample (T_1) and the holder (T_2), for comparison. Solid lines correspond to a small value of R_1 , where they are both at nearby temperatures; dashed lines correspond to a large value of R_1 , in which case the temperatures differ considerably.

To describe **cooling** the same Eqs. (3a,b) are used, with $q=0$, and the following initial conditions: If $\tau = 0$, then the initial values of T_1 and T_2 are T_{10} and T_{20} , respectively. The solutions are:

$$\left. \begin{aligned} T_1 &= T_\infty + M e^{m_1 \tau} + N e^{m_2 \tau} \\ T_2 &= T_1 + \frac{M m_1}{K_1} e^{m_1 \tau} + \frac{N m_2}{K_1} e^{m_2 \tau} \end{aligned} \right\} \tag{8a,b}$$

where m_1 and m_2 have the same values (Eq. 6 a,b), but M and N are now:

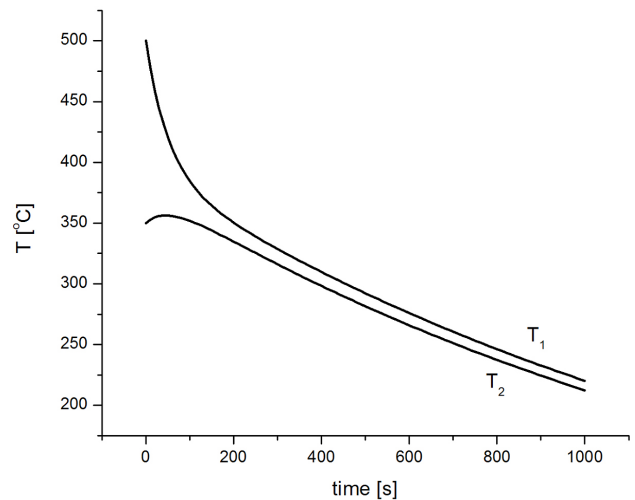


FIGURE 10. Calculated cooling of sample (T_1) and holder (T_2) when the sample is initially at a higher temperature than the holder.

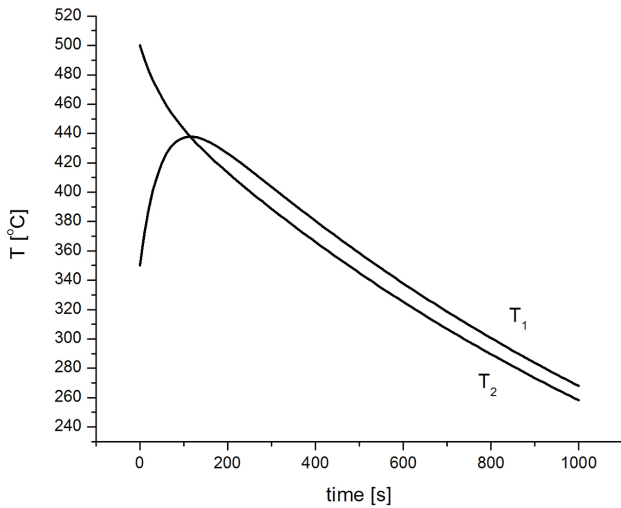


FIGURE 11. Calculated cooling of sample (T_1) and holder (T_2) when the sample is initially at a lower temperature than the holder.

$$\left. \begin{aligned} M &= \frac{K_1}{m_1 - m_2} \left[T_{20} - T_{10} - \frac{m_2}{K_1} (T_{10} - T_\infty) \right] \\ N &= T_{10} - T_\infty \\ &\quad - \frac{K_1}{m_1 - m_2} \left[T_{20} - T_{10} - \frac{m_2}{K_1} (T_{10} - T_\infty) \right] \end{aligned} \right\} \quad (9a,b)$$

Figure 10 shows the cooling of the sample and holder calculated if initially the sample is at a higher temperature, and Fig. 11 when the sample is initially cooler than the holder. In the first case (Fig. 10), as the sample cools, it initially transfers heat to the holder, and then they both cool down at

$$\left. \begin{aligned} m_1 &= \frac{-(K_1 + K_2 + K_3 + \frac{R_1}{R_0} K_1) + \sqrt{(K_1 + K_2 + K_3 + \frac{R_1}{R_0} K_1)^2 - 4K_1 \left[\frac{R_1}{R_0} (K_2 + K_3) + K_3 \right]}}{2} \\ m_2 &= \frac{-(K_1 + K_2 + K_3 + \frac{R_1}{R_0} K_1) - \sqrt{(K_1 + K_2 + K_3 + \frac{R_1}{R_0} K_1)^2 - 4K_1 \left[\frac{R_1}{R_0} (K_2 + K_3) + K_3 \right]}}{2} \end{aligned} \right\} \quad (13 a,b)$$

$$\left. \begin{aligned} M &= \frac{1}{m_1 - m_2} \left[\frac{q}{C_1} - T_\infty m_2 + K m_2 \right] \\ N &= T_\infty - K \\ &\quad - \frac{1}{m_1 - m_2} \left[\frac{q}{C_1} - T_\infty m_2 + K m_2 \right] \end{aligned} \right\} \quad (14 a,b)$$

Note that if $R_0 \rightarrow \infty$ the values of T_1 , T_2 , m_1 , m_2 , M and N reduce to the expressions of Eqs. (4-7).

With these values calculation were made for a stainless steel sample on an aluminium holder, shown in Fig. 12. Initially the sample heats up faster than the holder, but after some time the lines cross and the holder is at a higher temperature. This means that the sample is losing heat faster than the holder, through R_0 .

the same rate. In the opposite case (Fig. 11) the holder initially heats the sample, and then they both cool down at the same rate.

The only way that the sample can be cooler than the holder when the beam is removed is if the sample loses heat directly to the rest of the system. To consider this possibility a resistance R_0 was added in the equivalent circuit between points T_1 and T_∞ (see Fig. 5). It includes effects originally believed to be small and neglected. One is the thermocouple itself, whose two leads are a path for heat conduction. The other possible heat loss is by radiation. In the interval of interest here (see Fig. 2), we can assume heat loss by radiation to be approximately linear with temperature, so it may be included in R_0 . The radiative heat loss from the holder would be included in R_2 .

When the resistance R_0 is added, Eqs. (3a,b) become

$$\left. \begin{aligned} q &= \frac{1}{R_1} (T_1 - T_2) + C_1 \frac{\partial T_1}{\partial \tau} + \frac{T_1 - T_\infty}{R_0} \\ \frac{1}{R_1} (T_2 - T_1) + \frac{1}{R_2} (T_2 - T_\infty) &= -C_2 \frac{\partial T_2}{\partial \tau} \end{aligned} \right\} \quad (10a,b)$$

With the initial conditions if $\tau = 0$, $T_1 = T_2 = T_\infty$, the solution is

$$\left. \begin{aligned} T_1 &= K + M e^{m_1 \tau} + N e^{m_2 \tau} \\ T_2 &= T_1 + \frac{M m_1}{K_1} e^{m_1 \tau} \\ &\quad + \frac{N m_2}{K_1} e^{m_2 \tau} - q R_1 + \frac{R_1}{R_0} (T_1 - T_\infty) \end{aligned} \right\} \quad (11a,b)$$

where

$$K = T_\infty + \frac{R_1}{R_0} \left(\frac{K_2 + K_3}{K_3} \right) T_\infty + \frac{K_2 + K_3}{K_1 K_3} \frac{q}{C_1} \quad (12)$$

For the cooling stage the initial conditions are: if $\tau = 0$, $T_1 = T_{10}$ y $T_2 = T_{20}$. The solution is:

$$\left. \begin{aligned} M &= \frac{K_1}{m_1 - m_2} \\ &\quad \times \left[T_{20} - T_{10} - (T_{10} - T_\infty) \left(\frac{R_1}{R_0} + \frac{m_2}{K_1} \right) \right] \\ N &= T_{10} - T_\infty - \frac{K_1}{m_1 - m_2} \\ &\quad \times \left[T_{20} - T_{10} - (T_{10} - T_\infty) \left(\frac{R_1}{R_0} + \frac{m_2}{K_1} \right) \right] \end{aligned} \right\} \quad (15 a,b)$$

Equations (15a,b) reduce to Eqs. (9a,b) if $R_0 \rightarrow \infty$.

The main features of Fig. 4 are explained with the lumped heat capacity model:

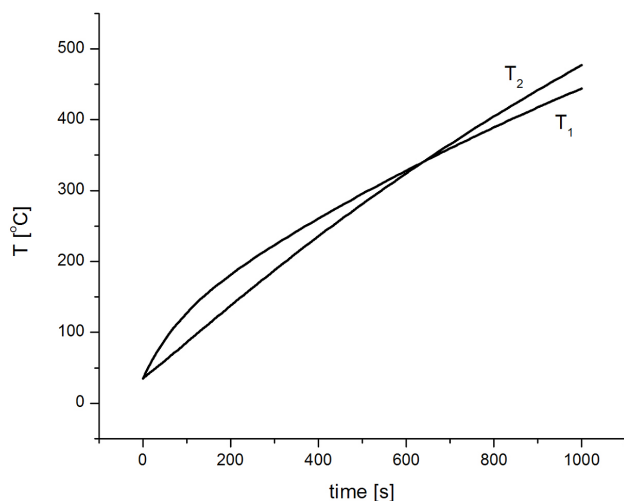


FIGURE 12. Calculated temperatures of sample and holder when R_0 is included, to simulate direct heat loss to the rest of the system. The curves cross over after a certain time.

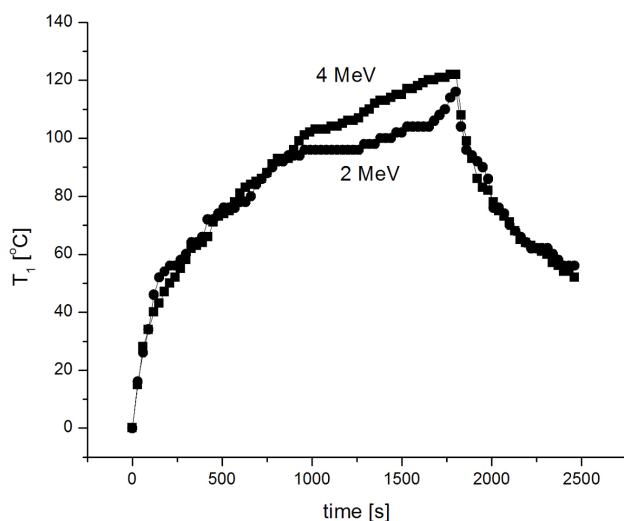


FIGURE 13. Test of linearity. An experiment done at 4 MeV and an experiment done at 2 MeV with values multiplied by 2.

- 1) In the initial stage curves A and C show a fast heating of the sample, with R_1 large; the slope is determined by the value of C_1 . In curve B with conducting silver paint R_1 is small, and sample and holder are heated together.
- 2) After about 100 seconds the whole system is heated in all cases, curve C rising slower due to the high value of C_2 .
- 3) In the initial stage of cooling curve A falls rapidly, as the sample cools faster than the holder. In curve B they both cool together due to a small value of R_1 . In curve C the sample is at a lower temperature than the holder, due to R_0 , so in the cooling stage it initially takes heat from the holder, and then both cool down.

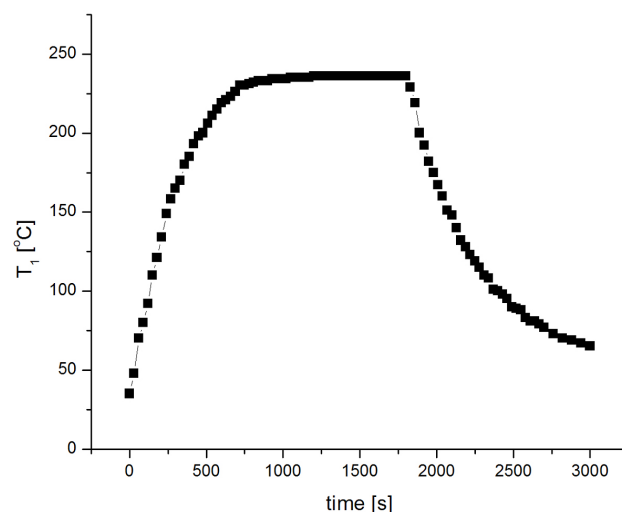


FIGURE 14. Temperature evolution of a sample on a totally insulated (except for the thermocouple) Teflon mounting.

- 4) In the final stage of cooling the rate of both sample and holder is determined by the value of R_2 .

The linearity of temperature behavior with the energy deposited q was studied. An experiment with a 4 MeV beam is compared with another experiment with a 2 MeV beam, but with the values multiplied by 2. All other conditions were kept the same (mount A). As Fig. 13 indicates, linearity is acceptable over most of the range, although in one case the beam was unstable. In another case, with mount C, linearity was lost.

Tests were made with a different mounting D, in which the sample was not in contact with any metal part, except for the thermocouple; the complete holder, including the flaps, were made of Teflon. A rapid rise in temperature and then a leveling off were observed, as Fig. 14 shows. This behavior was reproduced in a calculation with a value of $R_0 = 10 R_1$.

6. The values of the parameters

In the application of the lumped heat capacity model the parameters of interest are R_0 , R_1 , R_2 , C_1 and C_2 . Of these, $C_1 = \rho_x c_1 V_1$ and $C_2 = \rho_y c_2 V_2$ may in principle be known, since they contain the density, the specific heat and the volume of the sample and the holder, respectively. On the other hand, R_0 , R_1 and R_2 are unknown. R_0 is the resistance which represents the thermocouple leads and radiation loss from the sample. R_1 is the contact resistance between the sample and the holder, which can be reduced with conducting paint. Finally, R_2 contains the resistance between the holder and the rest of the system, plus radiation losses, and is difficult to control.

To illustrate the importance of these parameters, an experiment was repeated on different dates, which meant removing and then mounting the sample again. All conditions were reproduced (mount A, type of beam and energy, beam current,

thermocouple), but the reproducibility was poor, indicating the importance of these parameters.

7. Conclusions

Measurements of heating and cooling of the surface of a metal sample during bombardment with a beam of particles from the Pelletron Accelerator showed that these processes depend strongly on the mounting of the sample on the holder. To explain this behavior the lumped heat capacity method of heat transfer was applied. The method uses an analogy with an electric circuit, and is applicable to small metallic

samples. The development of heating and cooling with time, both of the sample and the holder, is explained in terms of the contact resistance between components and of properties of the materials (density, specific heat, volume). The behavior of several mountings was studied, and tests were made of linearity and reproducibility.

Acknowledgments

Thanks are due to R. Trejo, K. López, F Jaimes and M. Galindo for technical support.

-
1. H.S. Carslaw and J.C. Jaeger, *Conduction of Heat in Solids*, (Oxford University Press, 1959).
 2. J.P. Holman, *Heat Transfer* (McGraw- Hill Kogakusha, 1976).